PHILOSOPHICAL TRANSACTIONS B

rstb.royalsocietypublishing.org

Research

Cite this article: Rolfe RA, Shea CA, Singh PNP, Bandyopadhyay A, Murphy P. 2018 Investigating the mechanistic basis of biomechanical input controlling skeletal development: exploring the interplay with Wnt signalling at the joint. *Phil. Trans. R. Soc. B* **373**: 20170329.
http://dx.doi.org/10.1098/rstb.2017.0329

Accepted: 14 August 2018

One contribution of 14 to a Theo Murphy meeting issue 'Mechanics of Development'.

Subject Areas:
developmental biology

Keywords:
mechanical forces, molecular mechanisms, Wnt signalling, joint formation, electroporation, transgene expression

Author for correspondence:
Paula Murphy
e-mail: paula.murphy@tcd.ie

†These authors contributed equally to this work.

Electronic supplementary material is available online at http://dx.doi.org/10.6084/m9.figshare.c.4206887.

THE ROYAL SOCIETY PUBLISHING

Investigating the mechanistic basis of biomechanical input controlling skeletal development: exploring the interplay with Wnt signalling at the joint

Rebecca A. Rolfe[1,†], Claire A. Shea[1,†], Pratik Narendra Pratap Singh[2], Amitabha Bandyopadhyay[2] and Paula Murphy[1]

[1]Department of Zoology, School of Natural Sciences, Trinity College Dublin, The University of Dublin, Dublin, Ireland
[2]Department of Biological Sciences and Bioengineering, Indian Institute of Technology, Kanpur, Uttar Pradesh 208016, India

RAR, 0000-0003-2177-3136

Embryo movement is essential to the formation of a functional skeleton. Using mouse and chick models, we previously showed that mechanical forces influence gene regulation and tissue patterning, particularly at developing limb joints. However, the molecular mechanisms that underpin the influence of mechanical signals are poorly understood. Wnt signalling is required during skeletal development and is altered under reduced mechanical stimulation. Here, to explore Wnt signalling as a mediator of mechanical input, the expression of Wnt ligand and Fzd receptor genes in the developing skeletal rudiments was profiled. Canonical Wnt activity restricted to the developing joint was shown to be reduced under immobilization, while overexpression of activated β-catenin following electroporation of chick embryo limbs led to joint expansion, supporting the proposed role for Wnt signalling in mechanoresponsive joint patterning. Two key findings advance our understanding of the interplay between Wnt signalling and mechanical stimuli: first, loss of canonical Wnt activity at the joint shows reciprocal, coordinated misregulation of BMP signalling under altered mechanical influence. Second, this occurs simultaneously with increased expression of several Wnt pathway component genes in a territory peripheral to the joint, indicating the importance of mechanical stimulation for a population of potential joint progenitor cells.

This article is part of the Theo Murphy meeting issue 'Mechanics of Development'.

1. Introduction

It is well established that mechanical stimulation is important for multiple aspects of mature skeletal health, including fracture healing and bone remodelling [1]; however, a clearer picture of the influence of movement on embryonic skeletal development has only emerged recently [2–5] and its molecular basis remains incompletely understood. Spontaneous movement of the embryo commences early in development [6] and is an important source of mechanical stimulation for the forming skeleton. Evidence for this comes from human congenital disorders in which the absence or reduction of movement *in utero* results in skeletal anomalies including joint dysplasia and temporary brittle bones that are prone to fracture [7–9]. However, a more detailed characterization of the effects of reduced movement required the use of animal models, which demonstrated the precise events during development that depend on cues from movement (summarized in figure 1). These include the emergence of the correct rudiment shape (morphogenesis) [5], the initiation and progression of ossification

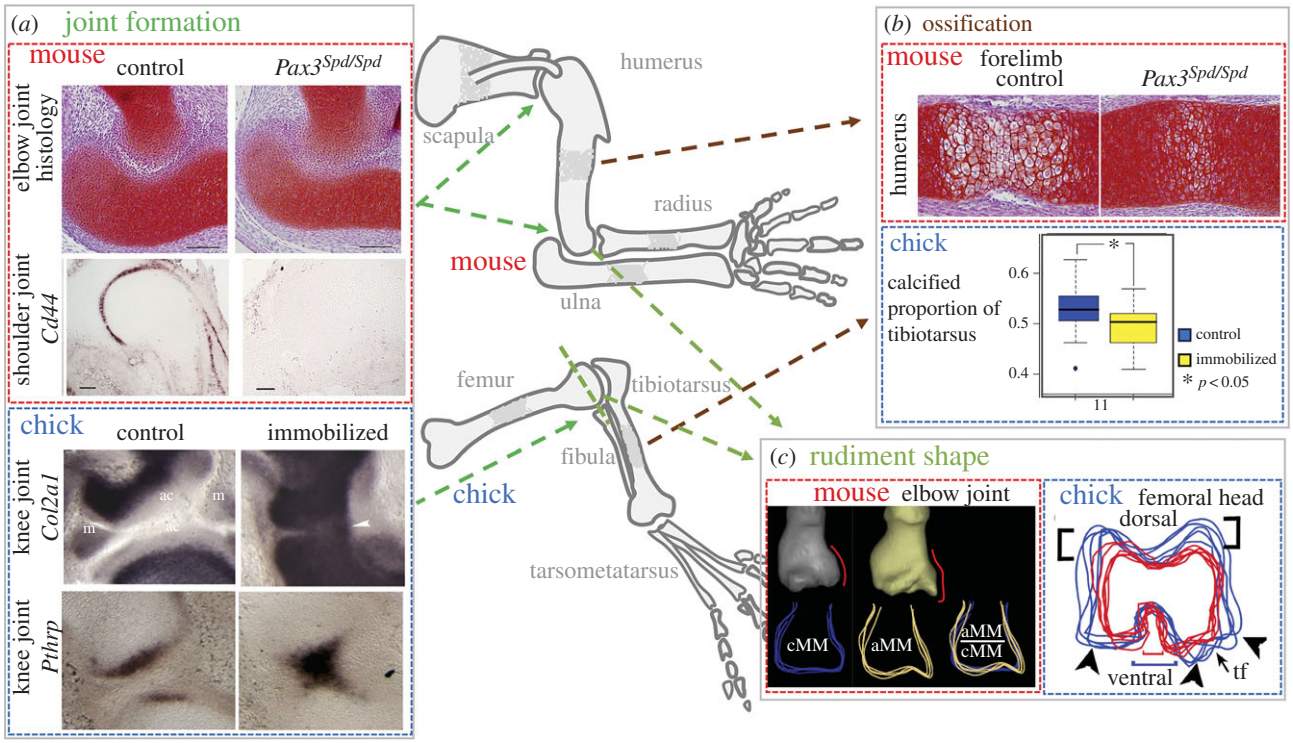

Figure 1. Lack of mechanical stimulation from movement has multiple phenotypic effects on limb skeletal development, observed in both mouse and chick immobilization models. Effects on joint formation (*a*), ossification (*b*) and rudiment shape (*c*) are shown in both the mouse forelimb (red boxes; TS23 (E14.5)) and chick hindlimb (blue boxes; HH35). Example data for each of (*a–c*) are shown in the boxes. (*a*) Joint formation. The elbow joint of the immobile mouse embryo (*Pax3*$^{Spd/Spd}$; red box; [10]) and knee joint of the chick embryo (decamethonium bromide treated; blue box; [5]) lack definition of joint territories, shown by histology (Safranin O) and the absence of joint marker gene (*Cd44*) expression as well as abnormal expression of *Col2a1* and *Pthrp* across the joint where joint fusion occurs. (*b*) Ossification. Histological sections show reduction in hypertrophy at the mid-diaphysis of the mouse humerus in *Pax3*$^{Spd/Spd}$ mutant embryos (muscle-less), compared with control [4]. Delayed ossification is similarly shown in the immobile chick (reduced proportion of mineralization) [11]. (*c*) Rudiment shape. The change in shape of the distal humerus in muscle-less, immobile mouse embryos (aMM) compared with control (cMM) (unpublished) and in the distal femur of immobilized chicks, shown by outlines of femoral head cross-sections of immobilized (*red*) and control (*blue*) embryos, overlaid [5]. m, meniscus; ac, articular cartilage; tf, tibiofibula.

[4,11,12] and the definition of tissue territories at the joint [3–5] (reviewed in [13–15]).

Synovial joint formation can be described with three distinct stages: specification of the joint site, differentiation of joint tissues and joint cavitation [16]. As joint tissues are differentiating, morphogenesis of the rudiments is simultaneously occurring [17]. Mouse and chick immobilization models show that the effects on joint development appear early, shortly after movement normally commences, and are complex, affecting the differentiation of joint-specific tissues (i.e. joint patterning) as well as the shapes of the rudiment termini [5]. Affected tissue territories include the menisci of the knee joint and the characteristic 'chondrogenous layers' that prefigure the articular cartilage of the joint. These changes in tissue differentiation correspond to loss of joint-specific gene expression (e.g. *Cd44* and *Gdf5*) and activation of ectopic expression characteristic of subchondral transient cartilage (e.g. *Col2a1*, *Pthrp*), leading to the observed 'fusion' of joints in immobilized specimens (figure 1*a*). Clearly, the distinction of cells that form the transient (*Col2a1*-positive) cartilage of the rudiment (future bone) from cells that form stable articular cartilage is crucial to the formation of a functional joint. Cell lineage analysis has shown that the joint zone is very dynamic, with contribution of cells from the adjacent territories of transient cartilage as well as from adjacent joint margin cells [18–20]. Ray *et al*. recently proposed a model of simultaneous differentiation of transient and articular cartilage [19]. Although it is not fully understood how distinct transient and articular cartilage territories are established and spatially maintained, mechanical stimulation from movement is required. However, little is known about the molecular mechanisms involved in interpreting mechanical signals and in generating a cellular response.

As an entry point into revealing the molecular changes that accompany the phenotypic effects of immobilization, we carried out a comparison of the transcriptomes of humeri and associated joints from muscle-less mutant (*Pax3*$^{Spd/Spd}$) and control littermate embryos at the developmental time point when abnormalities are first evident (Theiler Stage (TS) 23 (embryonic day (E) 14.5)) [10]. This revealed differential expression of 1132 genes and showed, in particular, strong disturbance of genes associated with the Wnt signalling pathway, corroborating the observation of reduced canonical Wnt reporter activity upon loss of limb movement [3,10]. Wnt signalling has also been implicated in responding to mechanical loading in the zebrafish jaw [21]. Indeed, both joint development and ossification are known to require carefully regulated Wnt signalling, indicating that the Wnt pathway might mediate multiple mechanosensitive processes [22–24]. Although specific Wnt ligand-encoding genes have been implicated in skeletal development, we do not have comprehensive knowledge of the Wnt pathway components involved. With regard to joint development, canonical Wnt signalling is crucial for the correct differentiation of articular cartilage, with disruption of the joint zone when the pathway is inactivated [23–25]. However, immobilization causes greater disturbance to the joint region than inhibition of Wnt signalling, suggesting that additional molecular mechanisms are involved in mediating the effects of mechanical stimulation on joint tissue patterning [26].

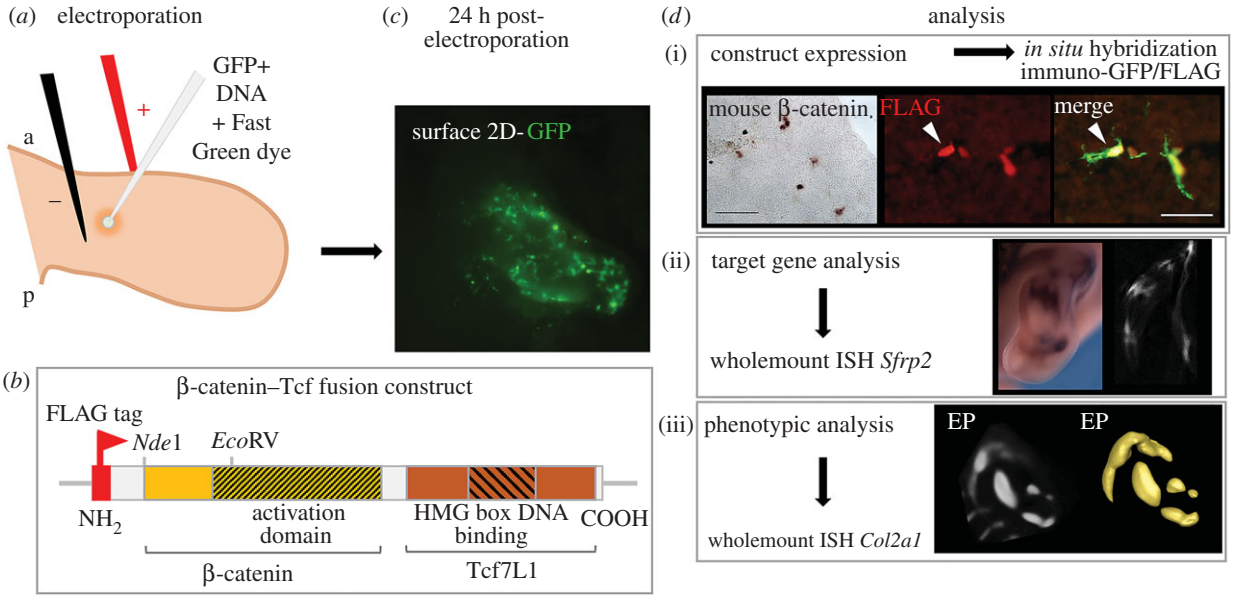

Figure 2. Experimental manipulation of Wnt signalling by *ex ovo* electroporation. Summary of experimental design and analysis pipeline used for manipulation of the Wnt signalling pathway. (*a*) Electroporation set-up; a, anterior; p, posterior. (*b*) Diagram of the expression construct fusing the β-catenin activation domain with the DNA-binding domain of Tcf7L1, incorporating a FLAG tag (GenBank KM189193) [32]. (*c*) GFP expression in whole limb 24 h post-electroporation. (*d*) Analysis pipeline: (i) expression of construct RNA by *in situ* hybridization (ISH) for mouse *β-catenin* (left) and fusion protein expression and nuclear localization through detection with anti-FLAG-tag antibody (middle), merged with GFP (right). (ii) ISH for *Sfrp2* RNA showed Wnt target gene upregulation at transgenic joints, and (iii) phenotypic analysis of the skeletal pattern in electroporated (EP) and control limbs, using *Col2a1* whole-mount ISH and 3D imaging by OPT. Scale bar, 50 µm.

Here, we expand our knowledge of the molecular signalling environment of the developing skeletal rudiment, in particular regarding Wnt signalling at the joint. We profile which Wnt ligand- and Fzd receptor-encoding genes are expressed within the developing forelimb skeleton in mouse during the period of sensitivity to movement (TS23 (E14.5)) and show that several component genes have localized expression in a territory peripheral to the joint. We show that canonical Wnt pathway activity, which is normally restricted to the developing joint region, is lost under immobilization, indicating that mechanical cues are required for the maintenance of Wnt activity and the joint territory. Exogenous activation of the canonical Wnt pathway in electroporated chick embryo limbs inhibited chondrogenesis and expanded the joint territory, corroborating the link between mechanically regulated Wnt signalling and joint definition. These findings indicate a key role for canonical Wnt signalling in interpreting and responding to biophysical stimuli generated by movement during joint development.

2. Material and methods

(a) Mouse lines

Heterozygous *Splotch delayed* (*Pax3*$^{Spd/+}$) mice [27] (Jackson Laboratories) were bred and euthanized under licence from the Irish Medicines Board/Health Products Regulatory Authority. *Splotch delayed* (*Pax3*$^{Spd/Spd}$) muscle-less mutant embryos were precisely staged (Theiler Stage [28]), fixed and dehydrated. Genotype was confirmed by PCR amplification [29].

Embryos from the *TCF/Lef:H2B-GFP* reporter mouse line [30] were kindly provided from the MRC Human Genetics Unit, Edinburgh, UK.

(b) *Ex ovo* chick embryo culture and limb bud electroporation

Fertilized chick eggs were obtained from Allenwood Broiler breeders Ltd (strain: Ross 503) and incubated (Natureform Hatchery UT350N) at 37°C for 72 h prior to transfer to *ex ovo* culture modelled on Schomann *et al.* [31]. On embryonic day (E)5, embryonic membranes were opened to expose the forelimb bud, which was microinjected with a mixture of Fast Green dye (0.5 µl of a 0.05% solution), and 1 µg each of pEGFP-C1 (BD Clontech 6084-1; GenBank accession no. U55763) and a construct encoding a constitutively active β-catenin–Tcf fusion protein with a FLAG tag (GenBank accession no. KM189193) (figure 2*b*). Control (sham) electroporated forelimb buds were microinjected with the same mixture replacing the β-catenin–Tcf fusion construct with phosphate-buffered saline (PBS). Plasmid DNA was sequence-verified and purified using a plasmid extraction kit (Qiagen 12163). Microinjection at the centre of the limb bud (figure 2*a*) was performed using a sterile, pulled capillary (borosilicate glass OD 1.0 mm, in a Sutter Instrument puller P-97) followed immediately by an optimized electroporation regime of six 60 ms pulses of 25 V, at an interval of 100 ms. Dulbecco's modified Eagle's medium (DMEM) culture medium, 1× antibiotic–antimycotic (Gibco 15240096) and less than 1 g of ground eggshell were added. The *ex ovo* set-up was incubated until harvest at E6. Embryo viability was recorded. Hamburger and Hamilton (HH) staging [33] was performed at the time of electroporation and at harvest. Electroporation efficiency was assessed by visualizing green fluorescence protein (GFP) under a fluorescence dissecting microscope immediately post-harvest (figure 2*c*). Specimens were fixed overnight in 4% paraformaldehyde in PBS, washed, dehydrated and stored at −20°C for analysis.

To assess construct uptake and expression, mouse *β-catenin* probe detected RNA and anti-FLAG antibody detected fusion protein products. Co-localization of GFP and the FLAG tag (using an anti-FLAG antibody) confirmed nuclear localization of the fusion protein (figure 2*d*). Canonical Wnt target gene expression and phenotypic analysis were assessed through whole-mount *in situ* hybridization for *Sfrp2* and *Col2a1* followed by optical projection tomography (OPT) three-dimensional (3D) imaging (figure 2*d*).

(c) *In situ* hybridization

Antisense RNA probes were generated from specific sequence-verified cDNA clones (electronic supplementary material, table S1). Hybridization of 60 µm vibratome sections, 10 µm cryosections or whole embryos was carried out largely as described previously [2,10,34].

(d) Optical projection tomography, image collection and processing

Following *in situ* hybridization, samples were prepared for OPT scanning and reconstruction as previously described [34].

(e) Histological staining

Mouse and chick embryonic limb paraffin sections (10 µm) were dewaxed and rehydrated. Nuclei were stained with Weigert's iron haematoxylin solution in 95% ethanol (1 min) and rinsed with running tap water. Safranin O staining was with Fast Green solution (0.001% in H_2O, 5 min), rinsed with 1% acetic acid and counterstained with Safranin O (0.1% in H_2O, 5 min). Mallory's Trichrome staining was performed with acid fuchsin (0.1% in H_2O, 5 min) and phosphotungstic acid (1% in H_2O, 10 min), and rinsed and stained in Aniline Blue (0.5% Aniline Blue, 2% Orange G and 2% oxalic acid in H_2O, 30 s).

(f) Immunohistochemistry

Limbs were rehydrated and either cryoprotected in 30% sucrose in PBS and frozen for cryosectioning, or paraffin-embedded and sectioned. Enzyme-mediated antigen retrieval was performed for pSMAD1/5/8 immunolabelling with 20 µg ml^{-1} proteinase K in 0.1 M Tris-HCl (Roche) for 10 min at 37°C. Sections were blocked for 30 min in 5% goat serum in Tris-buffered saline (TBS) with 0.1% Tween (TBST). Primary antibody was applied overnight at 4°C. Primary and secondary antibodies are listed in electronic supplementary material, table S1. Fluorescent samples were mounted with ProLong Gold Antifade Reagent with 4′,6-diamidino-2-phenylindole (DAPI; Life Technologies) and mounted in Mowiol with 2.5% 1,4-diazabicyclo[2.2.2]octane (DABCO; Sigma).

3. Results

(a) Wnt and Fzd gene expression during the period of early sensitivity to movement

The Wnt signalling pathway is complex, with multiple alternative ligands and receptors encoded by large gene families. To assess which Wnt ligand and Fzd receptor components are present within mechanosensitive tissues of the developing skeletal rudiment at the time of sensitivity, we analysed previously generated and verified transcriptomic data (ArrayExpress E-MTAB-1745 and E-MTAB-1746; [10]) for the developing humerus and associated joints of mouse at the earliest time point when phenotypic effects of immobilization are clearly observed (TS23 (E14.5)). Transcripts for 11 out of 19 Wnt ligand-encoding genes and all 10 Fzd receptor genes (*Fzd1–10*) were detected (average read count greater than 5) (figure 3*a*). Among Wnt genes, *Wnt5a* was by far the most abundantly expressed, with relatively high levels of *Wnt5b*, *Wnt9a*, *Wnt11* and *Wnt4* transcripts; all are genes previously associated with skeletal development [22,35–37]. The more surprising finding was similarly detectable levels of *Wnt2* and *Wnt2b* transcripts in the normal transcriptome, upregulated in the immobile mutant (figure 3*a*).

The transcriptomic data indicated which Wnt and Fzd genes are expressed and the relative levels of expression in the skeletal rudiments at this time. To reveal the spatial localization and relationship with tissues that are sensitive to alterations of movement, we carried out *in situ* hybridization for genes with the highest read counts. This revealed localized expression of *Wnt4*, *Wnt5a*, *Wnt9a* and *Wnt11* at the joints (figure 3*b*; shoulder and digit joints shown); while *Wnt9a* and *Wnt11* are expressed through the chondrogenous layers of the joint line (figure 3*b*; red arrows), *Wnt4* and *Wnt5a* are more localized to peripheral aspects.

Wnt2 and *Wnt2b* were not detected in the joint, but are expressed through the hypertrophic zone with high levels of *Wnt2* in the adjacent perichondrium/periosteum (figure 3*b*). *Wnt5a* showed faint expression in the pre-hypertrophic chondrocytes of the humerus, extending into the territory of the proliferative chondrocytes, while stronger *Wnt5b* expression was limited to the pre-hypertrophic zone (figure 3*b*, red arrows). Note that *Wnt2*, *Wnt2b*, *Wnt4* and *Wnt16* are expressed at significantly higher levels in muscle-less (immobile) humeri ($^*p \leq 0.05$; figure 3*a*).

Transcripts of all 10 Fzd genes were detected in RNA extracted from E14.5 mouse humeri and generally at higher levels than Wnt genes (figure 3*a*). However, using *in situ* hybridization, specific patterns of RNA localization were only detected for *Fzd3* and *Fzd6*, recording novel patterns for these genes in the joint region (figure 3*c*). Both genes were detected in the peripheral regions of both shoulder joints and elbow joints (figure 3*c*; black arrows), while *Fzd3* was also detected in the perichondrium of the scapula (green arrow) and *Fzd6* through the chondrogenous layers at the shoulder joint (red arrow).

(b) Canonical Wnt activity at the joint is lost in immobilized embryos while BMP signalling expands

The gene profiling work identified which Wnt and Fzd genes are active at the developing joint and can potentially contribute to Wnt activity. To directly assess Wnt pathway activity during the early period of sensitivity, embryos from the reporter mouse line *TCF/Lef:H2B-GFP* [30] were analysed (figure 4*a*). GFP-positive cells, indicative of canonical Wnt activity, are clearly visible in the muscle and ectoderm of the forelimb (figure 4*a*(i)). Canonical activity in joint cells is only visible at higher magnification (figure 4*a*(ii)), within the joint inter-zone (red arrow), in cells of the chondrogenous layers (square bracket) and in scattered cells in the subchondral zone of the rudiment (red arrowhead). Elsewhere in the rudiment, scattered GFP-positive cells are seen in the hypertrophic zone (figure 4*a*(iii)) and the perichondrium (not shown). Another indication of canonical Wnt activity in the mouse is nuclear accumulation of β-catenin (figure 4*b*), which corroborated the findings with the reporter mouse, showing enhanced staining at the joint line in wild-type embryos (figure 4*b*, left column, red arrows). In immobile $Pax3^{Spd/Spd}$ (muscle-less) forelimbs, detectable β-catenin protein is lost at both the shoulder and elbow joints (figure 4*b*, right column, red arrows). Contrastingly, perichondral detection of β-catenin and staining in scattered subchondral cells were not lost in muscle-less embryos (figure 4*b*, black arrows).

We have previously shown that BMP signalling is expanded across the joint in immobilized chick embryos and muscle-less mouse mutants ([26]; figure 4*c*). BMP activity, as detected by pSMAD1/5/8 immunoreactivity (both fluorescence and colorimetric), is observed across the articular region in the $Pax3^{Spd/Spd}$ muscle-less mutant mouse (figure 4*c*). Contrastingly, pSMAD1/5/8 is restricted to the subchondral cartilage at a distance from the joint line in wild-type littermates (figure 4*c*, green open bracket). In the mutant, there is no clear distinction between the chondrogenous layer and the subchondral territory

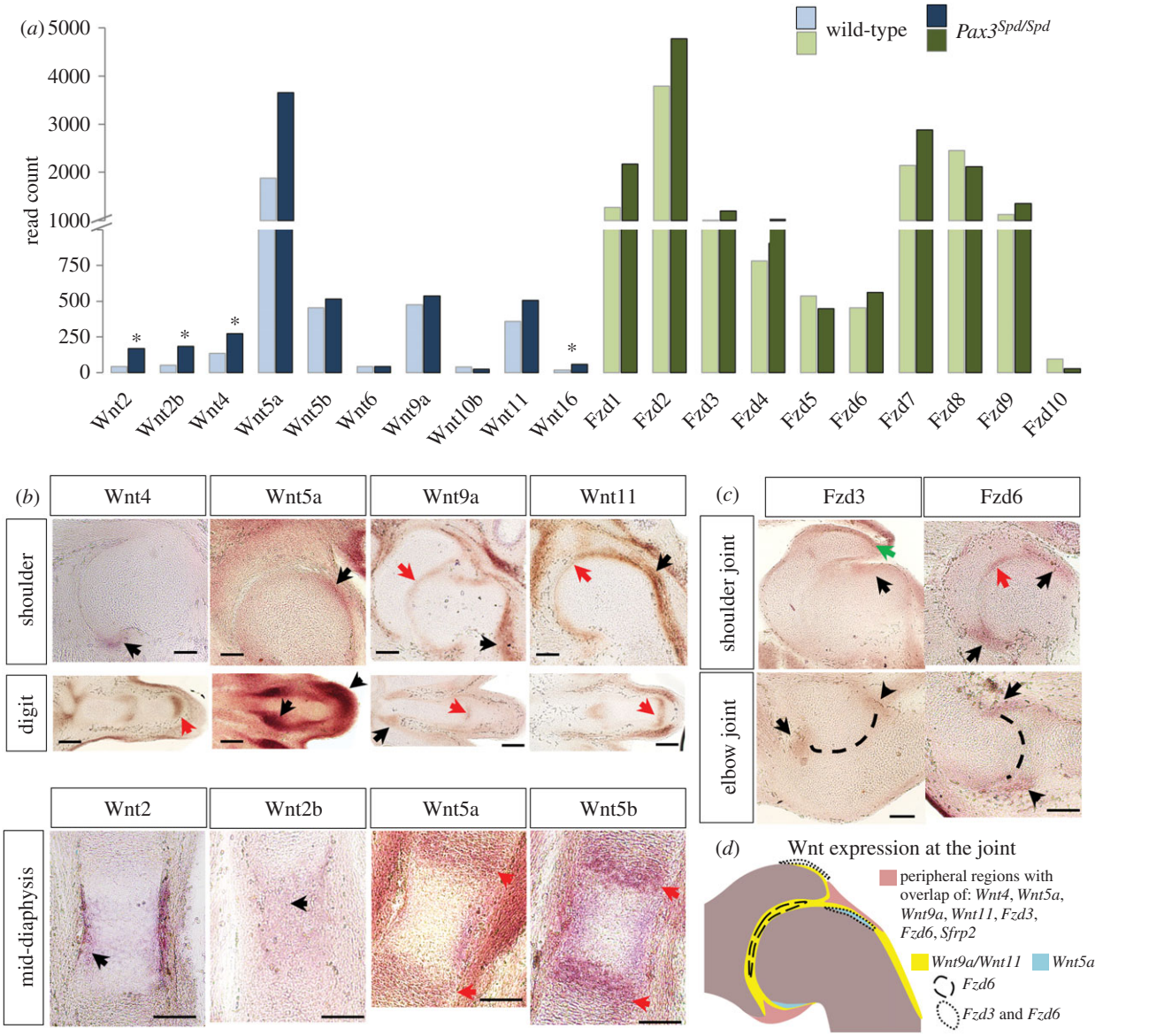

Figure 3. Wnt ligand and Fzd receptor-encoding genes are expressed during the early period of sensitivity to movement. (*a*) Relative expression levels (read counts) in the developing humerus and associated joints at TS23 (E14.5) in wild-type and *Pax3*$^{Spd/Spd}$ muscle-less mutants identified by RNA sequencing (RNA-seq) ($n = 3$); (*, differentially expressed, $p \leq 0.05$). Note that two different scales are represented on the *y*-axis, below and above 1000 reads, as indicated. (*b*) Wnt ligand genes are expressed in wild-type shoulder and digit joints and the mid-diaphysis of the humerus as indicated. Black arrows indicate expression localized peripheral to the joint; red arrows indicate expression through the joint line. Lower panel, mid-diaphysis; black arrows indicate expression in the hypertrophic zone with strong *Wnt2* expression in the adjacent perichondrium/periosteum. Red arrows indicate the pre-hypertropic zone. (*c*) *Fzd3* and *Fzd6* are expressed peripheral (black arrows) to the shoulder and elbow joint, and *Fzd6* within the joint line (red arrow); dashed lines indicate elbow joint line. *Fzd3* is also expressed in the perichondrium of the scapula (green arrow). (*d*) Schematic summarizing Wnt pathway component gene expression in the joint. Scale bars, 100 µm.

seen in the normal joint (figure 4*c*; orange bracket), together with expansion of the territory of BMP activity across the joint region (figure 4*c*, right-hand columns). Taken together, these data reveal that the absence of movement leads to a loss of canonical Wnt activity at the joint line, and a simultaneous expansion of BMP activity across the joint territory, indicating a reciprocal relationship between regulation of these two key signalling pathways, coordinated by movement.

(c) Ectopic activation of the canonical Wnt pathway inhibits chondrogenesis and enlarges the joint territory

Canonical Wnt activity is reduced in the developing shoulder and elbow joints in response to immobilization while joint tissues are mis-specified, resulting in partial cartilage fusion across the joint [4,5]. A number of mouse mutant lines show that reducing canonical Wnt signalling at the joint also leads to joint fusions, albeit with milder phenotypes than immobilization [23,24]. To further test the functional relationship between altered canonical Wnt activity and joint mis-specification, we sought to over-activate canonical Wnt signalling, with particular focus on the joint. We predicted that over-activation would result in an expanded joint territory. To over-activate canonical Wnt, we microinjected and electroporated an expression construct encoding a constitutively active form of the essential pathway mediator β-catenin (β-catenin–Tcf fusion protein, into chick forelimb; figure 2*b*). The fusion protein is capable of binding to the control regions of canonical Wnt pathway target genes and activating expression independent of signal transduction (β-catenin stabilization). The construct was

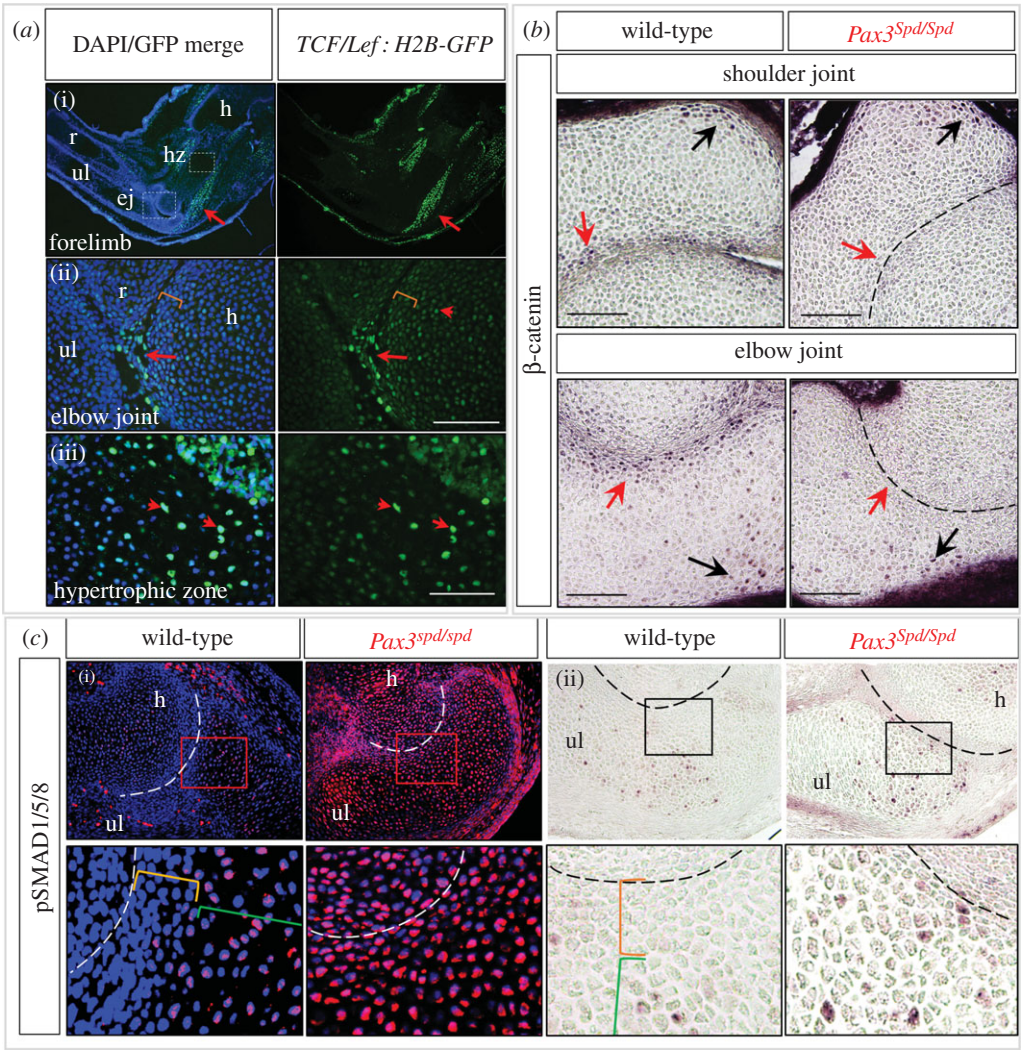

Figure 4. Canonical Wnt activity is altered at the forming joint in muscle-less embryos, coordinated with altered BMP signalling. (*a*) Cryosections of TS23 forelimbs from *TCF/Lef : H2B-GFP* reporter mice, showing canonical Wnt pathway activity (GFP) in the muscle and ectoderm of the forelimb (i), and in higher-magnification views at the elbow joint (ii), and hypertrophic zone (iii). Red arrows/arrowheads indicate GFP-positive cells; orange brackets indicate chondrogenous layers. (*b*) Immunolocalization of β-catenin in paraffin sections of wild-type and *Pax3*$^{Spd/Spd}$ mutant shoulder and elbow joints as indicated; presence or absence of detectable β-catenin (red arrows) at the joint line (dashed line). Black arrows indicate detection in scattered cells adjacent to the joint and perichondrium. (*c*) Fluorescence (i) and colorimetric (ii) immunolocalization of pSMAD1/5/8 in the wild-type and *Pax3*$^{Spd/Spd}$ mutant elbow joint (dashed line indicates joint line). Red and black boxes in the top row indicate regions of higher magnification shown in the bottom row. Orange brackets indicate the chondrogenous layers/presumptive articular cartilage in the normal joint; green open brackets indicate part of the subchondral territory. Note the absence of these zones and expansion of pSMAD1/5/8 activity in the mutant. Also note that, in (*c*), fluorescence detection of pSMAD1/5/8 is more sensitive than colorimetric detection. Scale bars, 100 µm. ej, elbow joint; hz, hypertrophic zone; h, humerus; r, radius; ul, ulna.

verified to activate reporter gene activity under TCF/Lef-binding site control in transient transfection assays (not shown); the fusion protein is localized to the nucleus in electroporated limb bud cells (figure 2*d*) and leads to increased expression of the target gene *Sfrp2* at the joints of electroporated limbs (figure 5*c*). The construct was co-electroporated with a GFP-encoding plasmid into the right forelimb of 124 chick embryos at E5 in *ex ovo* culture in 23 independent experiments. To examine the effect of expression of the β-catenin–Tcf fusion protein on the pattern of skeletogenesis, expression of the collagen type 2 alpha 1 (*Col2a1*) gene was detected by *in situ* hybridization, OPT scanned and reconstructed in three dimensions (figure 5). For comparison, the normal skeletal pattern was examined across stages HH26–HH30 (E5–E7) (figure 5*a*; electronic supplementary material, movie S1 and figure S1). The skeletal pattern was examined in limbs electroporated with the β-catenin–Tcf fusion protein (experimental limbs) (figure 5*d*), in control limbs sham-electroporated with the GFP-expressing construct only (figure 5*b*) and in contralateral non-electroporated limbs of each embryo, 24 h post-electroporation (figure 5*d*). GFP visualization revealed targeted cells and showed wide variation in their location and extent (figure 5*d* (i, upper images)). The sham-electroporated limbs showed no difference in the stage or pattern of skeletogenesis compared with contralateral control limbs in each case (figure 5*b*; electronic supplementary material, table S2), therefore confirming that electroporation alone was not responsible for the observed skeletal effects. A variety of alterations to the skeletal pattern were visible in chick embryos expressing β-catenin–Tcf fusion protein (figure 5*d*; electronic supplementary material, table S3). The alterations observed included the absence of entire skeletal rudiments (such as the radius and/or ulna missing in specimens 1 and 7; orange circles), interruptions within a rudiment (ectopic joints) (specimens 2 and 4; green arrowheads) and reductions in the size of skeletal elements (specimens 3, 5 and 6; red arrowheads) (figure 5*d*).

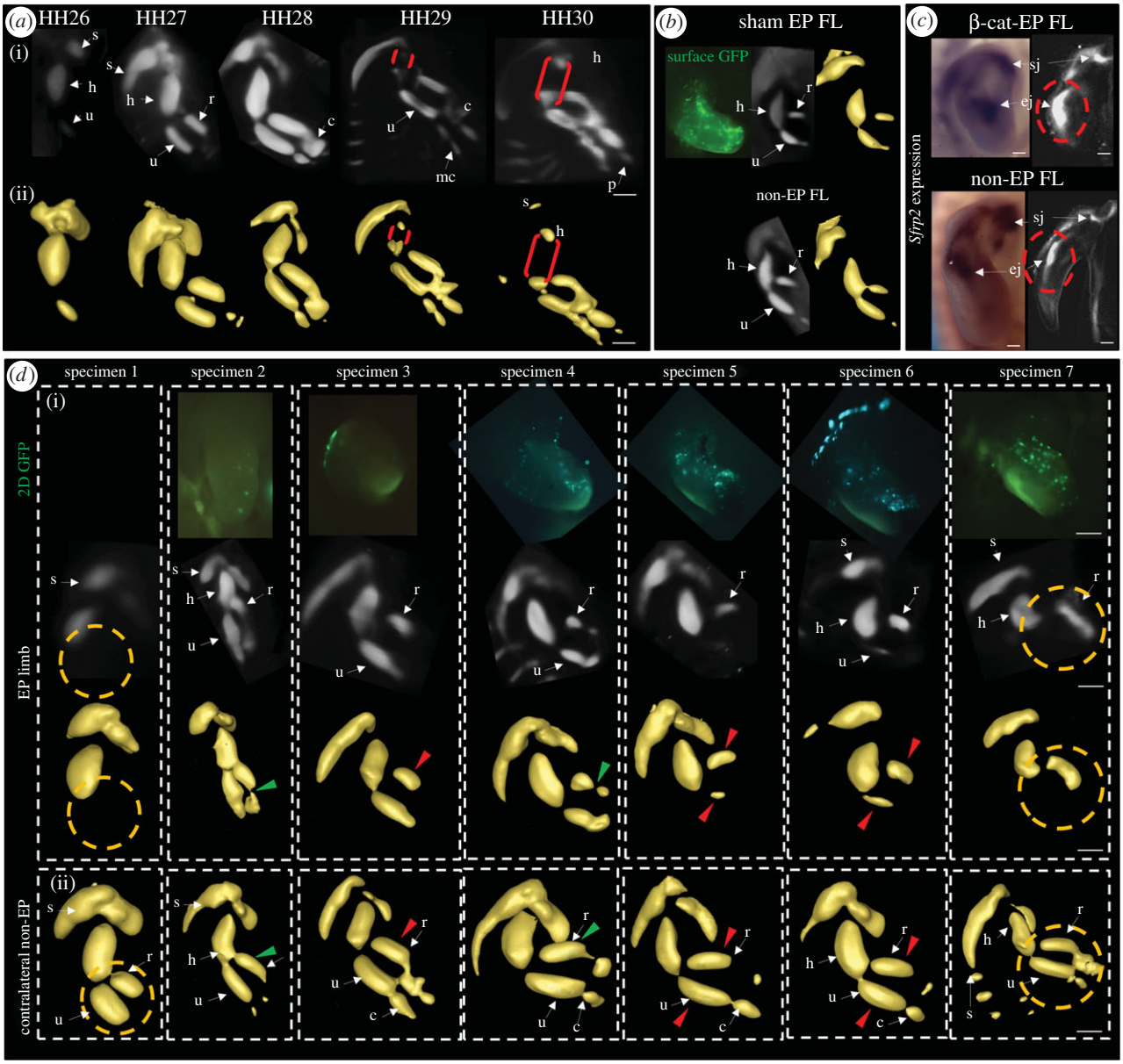

Figure 5. Increased activation of the canonical Wnt pathway inhibits chondrogenesis. (*a*) Three-dimensional analysis of the expression pattern of *Col2a1* in the developing forelimb across stages HH26–HH30 (E5–E7) reveals the normal pattern of chondrogenesis. Lateral views of volume-rendered 3D reconstructions following OPT scanning (expression appears white/grey) (i). Matching lateral views of surface-rendered data (expression shown in yellow) (ii). Red brackets show separation of *Col2a1*-expressing territories in the mid-diaphysis of the rudiment at HH29 and HH30, where hypertrophy is occurring. Scale bars, 200 µm. (*b*) Sham-electroporated specimens treated with PBS were compared with contralateral, non-electroporated limbs and showed no gross skeletal abnormalities, despite successful electroporation of the GFP reporter. (*c*) The Wnt target gene *Sfrp2* is upregulated at joints in electroporated limbs. Bright field (left) and 3D reconstructions (right) of *Sfrp2* expression in an HH27 non-electroporated (non-EP) forelimb (FL) and EP forelimb from the same specimen. Red ovals highlight upregulation of elbow joint *Sfrp2* gene expression. Scale bars, 100 µm. (*d*) Three-dimensional analysis of *Col2a1* expression in β-catenin–TCF fusion protein electroporated (EP) forelimbs (i) compared with contralateral non-electroporated (non-EP) limbs (ii) in seven independent specimens. Top row: two-dimensional GFP visualization of whole EP limbs shows the distribution of expressing cells. For each EP limb, the middle panels show lateral views of 3D reconstructions of *Col2a1* expression data, volume rendered following OPT scanning (expression appears white/grey). Lower elements are surface representations of *Col2a1* expression (yellow denotes expression territory). Orange circles indicate the observed absence of skeletal elements in EP limbs, in comparison with contralateral non-EP limbs. Note especially the absence of entire elements in specimens 1 and 7 (radius and/or ulna). Red arrowheads indicate reduced elements; green arrowheads, interrupted elements (compare EP and non-EP in each case). Scale bars, 200 µm. s, scapula; h, humerus; u, ulna; r, radius; c, carpal; mc, metacarpal; p, phalanges; sj, shoulder joint; ej, elbow joint.

In each case, the location and severity of the alteration grossly corresponded to the location and extent of exogenous expression, e.g. the mild alteration in specimen 3 corresponded to low GFP levels (figure 5*d*).

Specimens 5, 6 and 7 expressed β-catenin–Tcf fusion protein in the region of the elbow joint (figure 6*a–c*, respectively) or additionally in the shoulder joint (specimen 6; figure 6*b*). Enlargement of joint territories (separation between *Col2a1* expression) was seen in both elbow and shoulder joints expressing activated β-catenin fusion protein compared with control contralateral limbs (figure 6; compare electroporated (EP) limbs and non-EP limbs, red arrows), coincident with ectopic activation. All three specimens showed fusion construct expression in the elbow region coincident with joint expansion. The shoulder joints of two specimens show no difference in joint size (figure 6; yellow

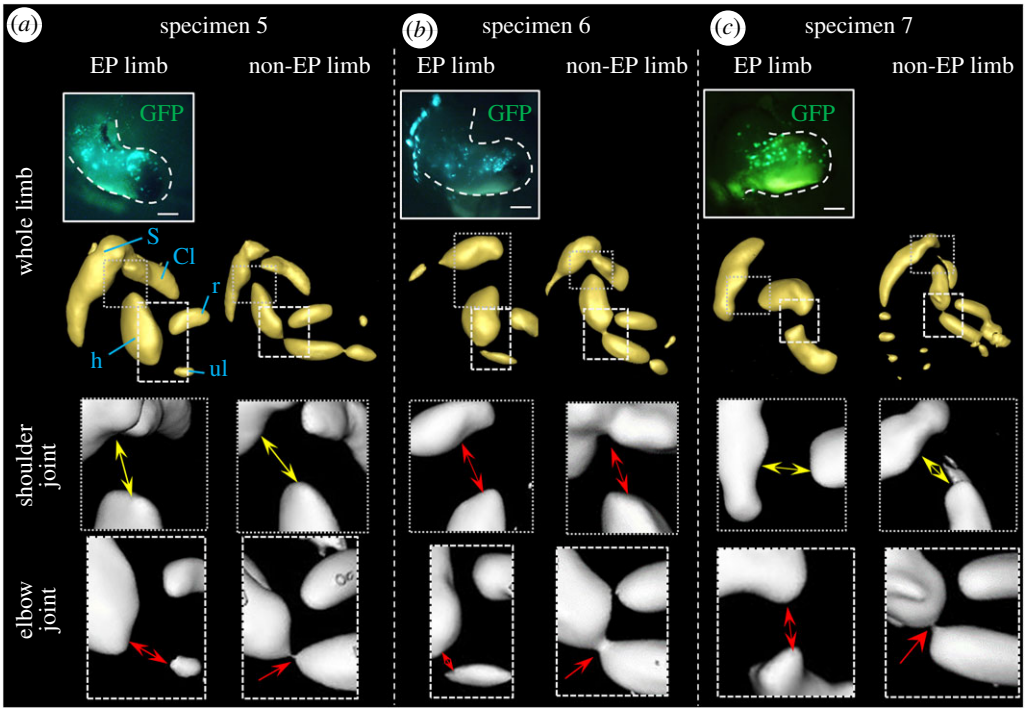

Figure 6. Ectopic activation of canonical Wnt signalling expands the joint region. Three-dimensional analysis of *Col2a1* expression in β-catenin–TCF fusion protein electroporated (EP) forelimbs in three independent specimens ((*a–c*); left column of each), compared with contralateral non-EP limbs (right column). Specimen numbers correspond to specimens presented in figure 5*d*. Whole-limb images of GFP expression in EP limbs show transgene expression (GFP); lateral views of surface representations of *Col2a1* expression domains following 3D OPT reconstructions for three specimens (yellow denotes expression territory). Higher-magnification boxes indicate shoulder and elbow joint regions in EP and non-EP limbs (white denotes expression territory). Red arrows in the joint space indicate expansion of the joint territory in the EP limb compared with the non-EP limb (distance between *Col2a1*-expressing elements). Yellow arrows indicate no difference in the joint. Scale bars, 200 μm.

arrows), but no GFP-positive cells were detected in the shoulder region. To ensure that whole-mount observations, as shown in figure 6, do not misrepresent joint spacing owing to the viewing angle, 3D data were analysed thoroughly through comprehensive virtual serial sections, which confirmed enlargement of the joint territories in each case (example shown in electronic supplementary material, figure S2). A corresponding expansion/upregulation of the expression domain of the Wnt target gene *Sfrp2* was also seen in the elbow joint region ($n = 2$) following β-catenin–Tcf fusion protein electroporation (figure 5*c*), further supporting the altered joint phenotype subsequent to Wnt pathway activation.

(d) Peripheral territories at the shoulder and elbow joints that express multiple Wnt pathway component genes are expanded in the muscle-less mutant

In the absence of movement, cells within the joint line ectopically express the transient cartilage marker *Col2a1* (figure 7*a*(i)), coincident with the loss of joint-specific markers [3,5], the loss of canonical Wnt pathway activity and the expansion of BMP activity. Also, it was clear from our gene expression analysis on mouse forelimb sections that multiple Wnt pathway component genes are expressed in territories peripheral to the elbow and shoulder joints: *Wnt4*, *Fzd3* and *Fzd6* in particular, but also partial overlap with *Wnt5a*, *Wnt9a* and *Wnt11* (cf. §3a), although no canonical Wnt activity was detected in these peripheral cells (cf. figure 4, and not shown). We previously showed expression of the Wnt modulator *Sfrp2* in peripheral cells [10]. We therefore sought to specifically examine changes in gene expression in these peripheral cells under reduced mechanical stimulation. In muscle-less mutant mouse embryos (*Pax3*$^{Spd/Spd}$), there is a clear increase in the expression of pathway components *Wnt4* and *Sfrp2* in the peripheral margins of the shoulder and elbow joints (figure 7*a*(ii,iii)) (upregulation verified by quantitative reverse transcriptase PCR (qRT-PCR); Wnt4 and Sfrp2, 4.5-fold in the sub-dissected elbow joint; Sfrp2, 3.38-fold in whole humerus). Further examination by histological staining in mouse forelimbs revealed an enlargement of the territory of peripheral cells in the muscle-less mutant compared with the wild-type, accompanied by an apparent increase in cellular density of this territory with immobilization (figure 7*b*). The absence of muscle in the mutant is clear and this joint peripheral region is negative for muscle- and tendon-specific antibody staining (not shown). The expansion of the territory, and of the expression of Wnt pathway components *Wnt4* and *Sfrp2* in this region, indicates the potential importance of these cells in aspects of Wnt-mediated control of joint development, impacted by mechanical stimulation from movement.

4. Discussion

Here we investigated a central role for Wnt signalling as a mediator of biophysical signals produced by embryo movement in the developing limb skeleton, particularly at the joint. We expand knowledge of which Wnt pathway component gene transcripts are localized in the joint and rudiment territories during the period of sensitivity to movement, using transcriptomic data to indicate the full catalogue of transcript levels and building on this using *in situ*

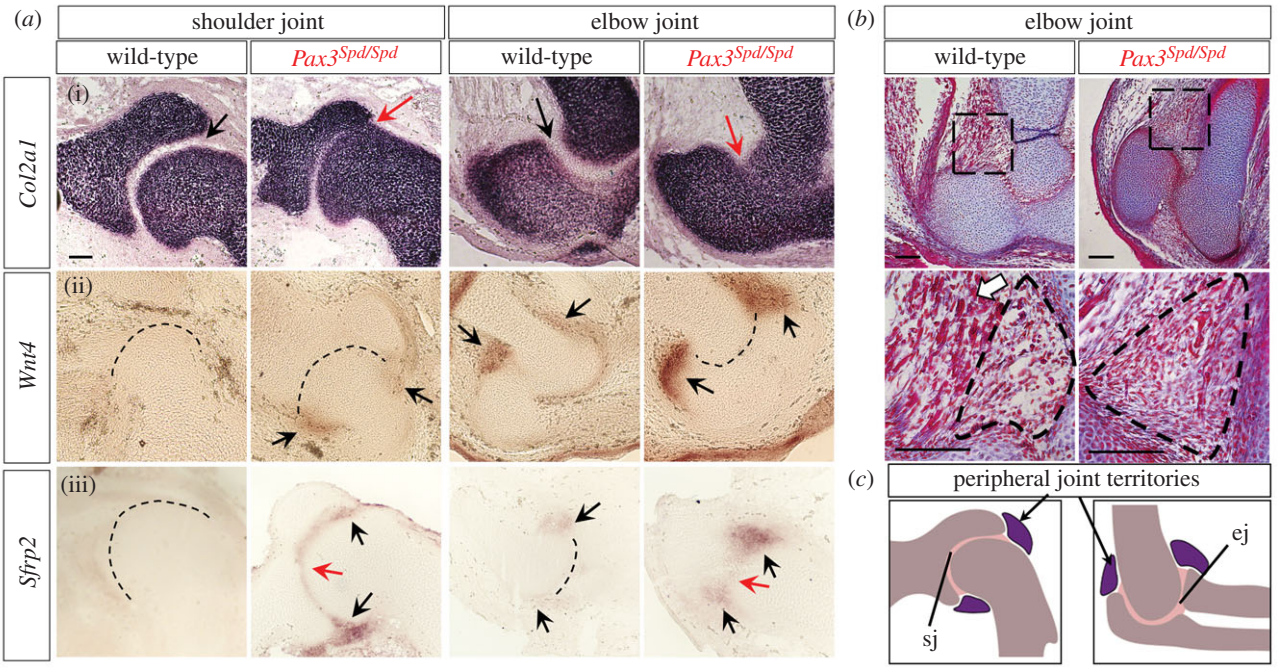

Figure 7. Increased/expanded expression of Wnt pathway component genes in the peripheral territory of the joint in muscle-less mutants. (*a*) Expression of the *Col2a1* gene (i) and of Wnt pathway components (*Wnt4* (ii) and *Sfrp2* (iii)) were compared in the shoulder and elbow joints of wild-type and *Pax3*$^{Spd/Spd}$ mutants at TS23. The mutant shows reduced separation of *Col2a1*-expressing territories at the shoulder and elbow (red arrows in (i)), compared with wild-type (black arrows in (i)). Upregulation of the expression of Wnt pathway genes *Wnt4* and *Sfrp2* was observed in tissue peripheral to the shoulder and elbow joints (black arrows in (ii); red arrows indicate joint line expression). (*b*) Histological staining using Mallory's Trichrome shows the peripheral territory of the elbow joint in wild-type and *Pax3*$^{Spd/Spd}$ mutants; outlines indicate regions shown in higher-magnification images in the bottom row. (*c*) Schematic indicating the peripheral joint territories in the shoulder (sj) and elbow joints (ej). Scale bars, 100 µm; scale bar on the first panel of (*a*(i)) is indicative of all in (*a*).

hybridization for the most abundantly expressed genes to reveal the relationship with tissue changes in the immobile mutant. In addition to previously known Wnts associated with the developing joint, it revealed novel expression of *Fzd3* and *Fzd6* at the developing joint and *Wnt2* and *Wnt2b* within the skeletal rudiment. The examination of spatial gene expression also highlighted, in particular, populations of cells at the peripheral margins of elbow and shoulder joints where several Wnt and Fzd genes are expressed in overlapping patterns, territories that are expanded in the immobile mutant. We show in greater detail which cells at the joint are actively responding to canonical Wnt signalling and the loss of this activity specifically at the joint line in the absence of limb movement, coincident with expansion of BMP signalling across the joint. This further illuminates the reciprocal relationship between mechanically regulated Wnt signalling and BMP signalling recently revealed [26]. Given the phenotype observed in immobile embryos of loss of joint-specific territories and fusion of *Col2a1*-expressing regions across the joint, concomitant with loss of Wnt signalling, we predicted that if Wnt is central to the immobilization phenotype, expansion of Wnt signalling would conversely lead to expansion of joint territories. We found this to indeed be the case when the pathway was ectopically activated in electroporated cells of the developing elbow and shoulder joints of the chick embryo. This provides functional evidence that supports the proposed role of canonical Wnt signalling in mediating mechanical regulation of tissue patterning at the limb joint.

Work to date has clearly demonstrated that mechanical stimulation generated by muscle contraction is required for multiple aspects of skeletal development (summarized in figure 1). It was previously shown that canonical Wnt pathway activity is generally downregulated at developing elbow joints of muscle-less mouse embryos [3], and we elaborate this finding using the GFP reporter mouse (*TCF/Lef:H2B-GFP* [30]) to show in more detail which cells are actively responding during the period of sensitivity. We find that, in immobile embryos, canonical Wnt pathway activity, reflected in nuclear β-catenin accumulation, is specifically lost within the interzone of the elbow and shoulder joints, while it is still detectable in scattered cells in adjacent territories, namely the perichondrium and subchondral rudiment. To further illuminate which components of the Wnt pathway machinery might be involved in interpreting these mechanical cues, we screened all Wnt- and Fzd-encoding genes for expression, at a time when the tissues are first sensitive to mechanical stimulation, revealing a number of novel findings. Firstly, all four Wnt2 and Wnt5 paralogous pairs of genes are expressed at and near the primary ossification site, opening the intriguing possibility that these duplicated gene pairs [38] have distinct but related functions during ossification; while Wnt5 paralogues have previously been shown to have distinct functions in chondrocyte proliferation and hypertrophy [22], Wnt2 genes have not previously been implicated. Wnt2 expression was detected in adult osteoblasts [39], but the novel description of *Wnt2* and *Wnt2b* expression at the hypertrophic zone and their increased level of expression in immobilized embryos implicates Wnt2 genes for the first time in endochondral ossification and specifically in its mechanoregulation.

It is striking that while Wnt ligand-encoding genes showed generally lower levels of transcripts than Fzd receptor-encoding genes in RNA extracted from the whole skeletal rudiment, specific Wnt genes are more readily detected in localized patterns of expression in the emerging tissues, indicating higher levels of expression in spatially restricted cells. Although transcripts for all 10 Fzd genes were present at

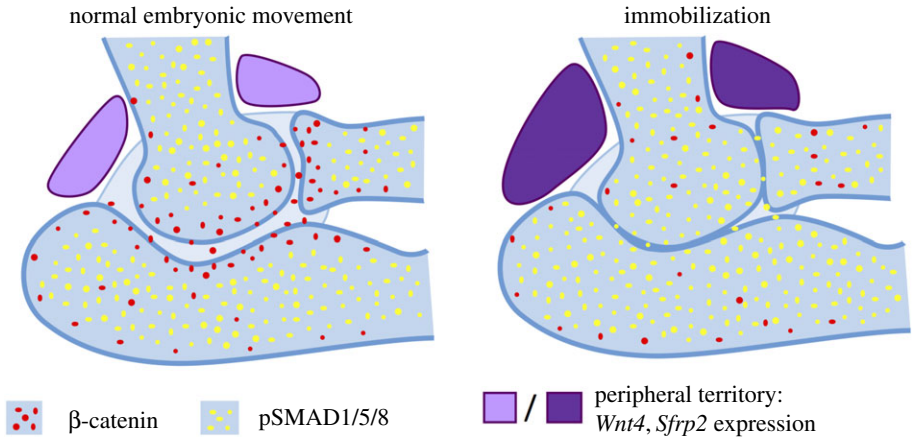

Figure 8. Schematic summarizing alterations at the elbow joint in immobile embryos, including altered Wnt and BMP signalling and expression of Wnt pathway genes in territories peripheral to the joint. With normal embryonic movement, canonical Wnt signalling (nuclear β-catenin) is localized largely to the joint line and future regions of articular cartilage as well as scattered cells in subchondral regions and at the perichondrium of each rudiment (red dots). BMP activity (pSMAD1/5/8) is detected at a distance from the joint line (yellow dots). With immobilization, articular zone β-catenin detection is specifically lost, and pSMAD1/5/8 detection spreads across the presumptive joint regions, where joint fusion occurs. In addition, a territory peripheral to the joint shows increased/expanded expression of Wnt pathway genes in immobile embryos, highlighting a possible impact on a source of joint progenitor cells.

relatively high levels, only *Fzd3* and *Fzd6* RNA was detectable in localized patterns, specifically at the joint, implicating these receptor-encoding genes for the first time in Wnt regulation of joint development. *Fzd3* was previously detected in mouse tibia at E18.5 and implicated in non-canonical Wnt/PCP regulation of chondrocyte proliferation [40] but not previously associated with joint development. We found that *Fzd6* is uniquely detected in the chondrogenous layers of the joint at this stage (figure 3*c*).

Another novel finding is the overlapping expression of several Wnt and Fzd genes in cells peripheral to the joint. Expression of *Wnt4* and *Sfrp2* is relatively extensive here, while *Wnt5a*, *Wnt9a*, *Wnt11*, *Fzd3* and *Fzd6* expression overlaps in more restricted domains (figure 3*d*). In muscle-less mutant mouse embryos, the expression of *Wnt4* and *Sfrp2* in these territories is increased and expanded, and histological staining indicated that the territory is enlarged in the mutant compared with the wild-type (figure 7). A number of studies have shown that cells migrate from outside the joint inter-zone after specification to contribute to joint tissues, in particular, lineage-tracing studies using DiI and fate mapping of *Col2a1*- and *Gdf5*-expressing cells [16,19,41,42]. A novel constant influx model of joint development was elaborated by Shwartz *et al*. [20] using a knock-in *Gdf5-CreER*^{T2} mouse and a range of tamoxifen pulse–chase timings in the joint over time. They noted the presence of *Gdf5*-expressing cells, initially outside the forming joint territory, and their subsequent contribution to the menisci, ligaments and epiphyseal and articular cartilages. This concept is also supported by surgical experiments where excision of a 'window' within the joint, leaving strips of adjacent tissue, can result in joint regeneration [43]. It is an attractive possibility that under reduced mechanical stimulation, peripheral cells fail to migrate to the joint territory, contributing to the immobilization phenotype (absence of joint-specific tissues). The expression of multiple Wnt pathway genes in the peripheral territory suggests that these cells might be primed to contribute to joint-specific Wnt signalling.

Precise spatial localization of Wnt and BMP signalling at the joint has previously been demonstrated, where BMP signalling is synonymous with transient cartilage formation of the skeletal rudiment and Wnt signalling is restricted to the future joint, where permanent articular cartilage forms [19]. We previously highlighted that while inactivation of canonical Wnt signalling at the joint leads to inappropriate expression of *Col2a1* [18,24], these phenotypes are less severe than the joint fusions observed in both mouse and chick following immobilization [26]. We therefore examined alteration to BMP signalling following immobilization and showed that whereas pSMAD1/5/8 is normally restricted at a distance from the joint, it spreads across the joint site in immobilized embryos. Here, we elaborate the impact of immobilization on the canonical Wnt pathway and show that activity is lost specifically in the joint, with activity maintained in the adjacent perichondrium and scattered cells in the subchondral region. Our previous computational modelling of biophysical stimuli generated by limb flexion/extension predicted peak levels of octahedral strain and stimulus at the extreme tips/joint interfaces of the humerus at TS23 [44] and dynamic cycles of hydrostatic pressure in the inter-zone [45]. Figure 8 summarizes the effects on Wnt and BMP signalling we observe at the elbow joint, emphasizing the reciprocal, coordinated effects on these essential signalling pathways. Although we as yet do not know the mechanism through which biophysical stimuli regulate these signalling outputs, we have identified particularly interesting candidate intermediaries through the genes that are dis-regulated following immobilization: while a negative regulator of Wnt signalling, *Sfrp2*, is strikingly upregulated at the joint line in immobilized embryos (figure 7), negative regulators of BMP signalling, *Smurf1* and *Smurf2*, are downregulated in subchondral regions [26]. We propose that the effects of immobilization on the joint are the result of multiple alterations in a coordinated system where contribution of progenitor cells from the periphery is disturbed as well as signalling activity within and close to the joint (figure 8).

Mechanical stimulation is required for the correct coordination of spatial territories of BMP and Wnt signalling activities at the joint, and while immobilization leads to joint fusions, hypermobilization causes joint expansion [46]. To further test a proposed central role for canonical Wnt signalling in the mechanically sensitive specification of joint tissues, we predicted that if canonical Wnt signalling was increased/

expanded at the joint, it would lead to joint enlargement. Using transient expression of a constitutively activated β-catenin fusion protein in the elbow or shoulder regions of electroporated chick embryos, we showed this to be indeed the case (figure 6). While it was challenging to precisely direct expression to the joint in these experiments, through monitoring the site of ectopic expression (GFP) and thorough phenotypic analysis of the whole emerging limb skeletal pattern using 3D imaging in large numbers of individual specimens, we confirmed the anti-chondrogenic effect when canonical Wnt signalling is activated within the rudiment (figure 5; [23]) and, in a number of specimens with ectopic activation specifically at the joint, we found expansion of the joint territory. This joint expansion is accompanied by increased expression of *Sfrp2* specifically in this region (figure 5*c*), corroborating the proposed central role of *Sfrp2* regulation (which is mechanosensitive, figure 7; [10]) in defining the joint territory. A priority for future work is further characterization of cellular and molecular characteristics within expanded joint regions following ectopic Wnt activation and hypermobilization [46]. Although technically challenging given the difficulty to specifically target ectopic activation to the joint, it would be interesting to test if we can rescue the immobilization phenotype through forced activation of canonical Wnt and how this has an impact on BMP/pSMAD activity to further explore the reciprocal relationship between the signalling pathways.

The chick limb electroporation studies were challenging in a number of respects, including the difficulty of precise spatial targeting and variability in the extent of transgene expression. This means that each individual embryo represents a unique situation. Nevertheless, the same finding of joint expansion upon transgene expression was repeated across all relevant specimens. DNA uptake and expression appeared to be achieved more readily in cells lying outside the condensed mesenchyme at the core of the limb bud (not shown), which is possibly a consequence of the stage at which electroporation was carried out (E5). Stable integration at earlier stages combined with the use of tissue-specific promoters may give better targeting of ectopic activation, making rescue experiments more feasible.

This experimental approach specifically explores the role of canonical signalling in the mechanically sensitive process of joint patterning; however, non-canonical Wnt signalling is also implicated through the expression of genes typically viewed as non-canonical, such as *Wnt5a* and *Wnt11*, two of the most highly expressed genes shown here. The non-canonical pathway has also been implicated in chondrocyte cell polarity and elongation of skeletal rudiments, shown to be affected by altered embryo movement [20,21]. While *Wnt5a* and *Wnt11* can affect both canonical and non-canonical signalling [47,48], interplay between different pathways needs further exploration.

In summary, this study shows that multiple aspects of joint patterning are affected when embryo movement is reduced or absent and furthers our understanding of the importance of Wnt signalling in interpreting the mechanical stimuli generated by movement for correct patterning of emerging joint tissues. Localized canonical Wnt activation at the joint is necessary for the elaboration of joint-specific tissues, which was corroborated by experiments expanding Wnt activity at the joint. We propose a model where mechanical stimulation is required for (i) the correct coordination of spatial territories of BMP and Wnt signalling activities which, when lost, leads to inappropriate tissue differentiation and (ii) influencing the contribution of progenitor cells to the joint from a peripheral territory (figure 8). The model fits with available data and will be an important basis for further investigation of the dynamics between major regulatory components: Wnt, BMP and mechanical stimuli.

Data accessibility. All data supporting this article are provided in the main text or as part of the electronic supplementary material. The datasets supporting the results of this article are available in the EMBL-EBI ArrayExpress repository (http://www.ebi.ac.uk/arrayexpress/), for the transcriptome (E-MTAB-1745) and differentially expressed dataset (E-MTAB-1746).

Authors' contributions. Conception and design: R.A.R., C.A.S. and P.M. Acquisition of data: R.A.R., C.A.S. and P.N.P.S. Analysis and interpretation: all authors. Writing the article: R.A.R., C.A.S. and P.M. Revising the article: P.N.P.S and A.B. Final approval for publication: all authors.

Competing interests. We declare we have no competing interests.

Funding. This work was supported by Trinity College Innovation bursaries (R.A.R. and P.M.), an Irish Research Council Postgraduate Studentship (GOIPG/2013/233) (C.A.S.), a European Molecular Biology Short-Term Fellowship (EMBO ASTF 175-2016) (C.A.S.), the Trinity College Faculty of Engineering Mathematics and Science India-Ireland scheme (P.N.P.S., P.M. and C.A.S.) and the Indian Ministry of Science (P.N.P.S. and A.B.).

Acknowledgements. We are grateful to Dr Chris Armit and Anna Thornburn, University of Edinburgh, UK for providing embryos from the *TCF/Lef:H2B-GTP* reporter line. We thank Catriona Daly and Roisín Joyce for contributing to optimization of the *ex ovo* chick culture and limb electroporation techniques.

References

1. Castillo AB, Leucht P. 2015 Bone homeostasis and repair: forced into shape. *Curr. Rheumatol. Rep.* **17**, 58. (doi:10.1007/s11926-015-0537-9)
2. Nowlan NC, Prendergast PJ, Murphy P. 2008 Identification of mechanosensitive genes during embryonic bone formation. *PLoS Comput. Biol.* **4**, e1000250. (doi:10.1371/journal.pcbi.1000250)
3. Kahn J *et al.* 2009 Muscle contraction is necessary to maintain joint progenitor cell fate. *Dev. Cell* **16**, 734–743. (doi:10.1016/j.devcel.2009.04.013)
4. Nowlan NC, Bourdon C, Dumas G, Tajbakhsh S, Prendergast PJ, Murphy P. 2010 Developing bones are differentially affected by compromised skeletal muscle formation. *Bone* **46**, 1275–1285. (doi:10.1016/j.bone.2009.11.026)
5. Roddy KA, Prendergast PJ, Murphy P. 2011 Mechanical influences on morphogenesis of the knee joint revealed through morphological, molecular and computational analysis of immobilised embryos. *PLoS ONE* **6**, e17526. (doi:10.1371/journal.pone.0017526)
6. Hamburger V. 1963 Some aspects of the embryology of behavior. *Q. Rev. Biol.* **38**, 342–365. (doi:10.1086/403941)
7. Moessinger AC. 1983 Fetal akinesia deformation sequence: an animal model. *Pediatrics* **72**, 857–863.
8. Rodriguez JI, Garcia-Alix A, Palacios J, Paniagua R. 1988 Changes in the long bones due to fetal immobility caused by neuromuscular disease. A radiographic and histological study. *J. Bone Joint Surg. Am.* **70**, 1052–1060. (doi:10.2106/00004623-198870070-00014)
9. Rodriguez JI, Palacios J, Garcia-Alix A, Pastor I, Paniagua R. 1988 Effects of immobilization on fetal bone development. A morphometric study in

newborns with congenital neuromuscular diseases with intrauterine onset. *Calcif. Tissue Int.* **43**, 335–339. (doi:10.1007/BF02553275)

10. Rolfe RA, Nowlan NC, Kenny EM, Cormican P, Morris DW, Prendergast PJ, Kelly D, Murphy P. 2014 Identification of mechanosensitive genes during skeletal development: alteration of genes associated with cytoskeletal rearrangement and cell signalling pathways. *BMC Genomics* **15**, 48. (doi:10.1186/1471-2164-15-48)
11. Nowlan NC, Murphy P, Prendergast PJ. 2008 A dynamic pattern of mechanical stimulation promotes ossification in avian embryonic long bones. *J. Biomech.* **41**, 249–258. (doi:10.1016/j.jbiomech.2007.09.031)
12. Rot-Nikcevic I, Reddy T, Downing KJ, Belliveau AC, HallgrÃmsson B, Hall BK, Kablar B. 2006 Myf5$^{-/-}$: MyoD$^{-/-}$ amyogenic fetuses reveal the importance of early contraction and static loading by striated muscle in mouse skeletogenesis. *Dev. Genes Evol.* **216**, 1–9. (doi:10.1007/s00427-005-0024-9)
13. Rolfe R, Roddy K, Murphy P. 2013 Mechanical regulation of skeletal development. *Curr. Osteoporos. Rep.* **11**, 107–116. (doi:10.1007/s11914-013-0137-4)
14. Shea CA, Rolfe RA, Murphy P. 2015 The importance of foetal movement for co-ordinated cartilage and bone development *in utero*: clinical consequences and potential for therapy. *Bone Joint Res.* **4**, 105–116. (doi:10.1302/2046-3758.47.2000387)
15. Felsenthal N, Zelzer E. 2017 Mechanical regulation of musculoskeletal system development. *Development* **144**, 4271–4283. (doi:10.1242/dev.151266)
16. Pacifici M *et al.* 2006 Cellular and molecular mechanisms of synovial joint and articular cartilage formation. *Ann. NY Acad. Sci.* **1068**, 74–86. (doi:10.1196/annals.1346.010)
17. Roddy KA, Nowlan NC, Prendergast PJ, Murphy P. 2009 3D representation of the developing chick knee joint: a novel approach integrating multiple components. *J. Anat.* **214**, 374–387. (doi:10.1111/j.1469-7580.2008.01040.x)
18. Koyama E *et al.* 2008 A distinct cohort of progenitor cells participates in synovial joint and articular cartilage formation during mouse limb skeletogenesis. *Dev. Biol.* **316**, 62–73. (doi:10.1016/j.ydbio.2008.01.012)
19. Ray A, Singh PN, Sohaskey ML, Harland RM, Bandyopadhyay A. 2015 Precise spatial restriction of BMP signaling is essential for articular cartilage differentiation. *Development* **142**, 1169–1179. (doi:10.1242/dev.110940)
20. Shwartz Y, Viukov S, Krief S, Zelzer E. 2016 Joint development involves a continuous influx of Gdf5-positive cells. *Cell Rep.* **15**, 2577–2587. (doi:10.1016/j.celrep.2016.05.055)
21. Brunt LH, Begg K, Kague E, Cross S, Hammond CL. 2017 Wnt signalling controls the response to mechanical loading during zebrafish joint development. *Development* **144**, 2798–2809. (doi:10.1242/dev.153528)
22. Yang Y, Topol L, Lee H, Wu J. 2003 Wnt5a and Wnt5b exhibit distinct activities in coordinating chondrocyte proliferation and differentiation. *Development* **130**, 1003–1015. (doi:10.1242/dev.00324)
23. Guo X, Day TF, Jiang X, Garrett-Beal L, Topol L, Yang Y. 2004 Wnt/beta-catenin signaling is sufficient and necessary for synovial joint formation. *Genes Dev.* **18**, 2404–2417. (doi:10.1101/gad.1230704)
24. Spater D, Hill TP, Gruber M, Hartmann C. 2006 Role of canonical Wnt-signalling in joint formation. *Eur. Cell Mater.* **12**, 71–80. (doi:10.22203/eCM.v012a09)
25. Kan A, Tabin CJ. 2013 c-Jun is required for the specification of joint cell fates. *Genes Dev.* **27**, 514–524. (doi:10.1101/gad.209239.112)
26. Singh PNP *et al.* 2018 Precise spatial restriction of BMP signaling in developing joints is perturbed upon loss of embryo movement. *Development* **145**, dev153460. (doi:10.1242/dev.153460)
27. Vogan KJ, Epstein DJ, Trasler DG, Gros P. 1993 The *splotch-delayed* (*Sp^{d}*) mouse mutant carries a point mutation within the paired box of the *Pax-3* gene. *Genomics* **17**, 364–369. (doi:10.1006/geno.1993.1333)
28. Theiler K. 1989 *The house mouse: atlas of embryonic development*. New York, NY: Springer-Verlag.
29. Keller-Peck CR, Mullen RJ. 1997 Altered cell proliferation in the spinal cord of mouse neural tube mutants curly tail and Pax3 splotch-delayed. *Dev. Brain Res.* **102**, 177–188. (doi:10.1016/S0165-3806(97)00095-3)
30. Ferrer-Vaquer A, Piliszek A, Tian G, Aho RJ, Dufort D, Hadjantonakis AK. 2010 A sensitive and bright single-cell resolution live imaging reporter of Wnt/β-catenin signaling in the mouse. *BMC Dev. Biol.* **10**, 121. (doi:10.1186/1471-213X-10-121)
31. Schomann T, Qunneis F, Widera D, Kaltschmidt C, Kaltschmidt B. 2013 Improved method for *ex ovo*-cultivation of developing chicken embryos for human stem cell xenografts. *Stem Cells Int.* **2013**, 960958. (doi:10.1155/2013/960958)
32. Duffy DJ *et al.* 2016 Wnt signalling is a bi-directional vulnerability of cancer cells. *Oncotarget* **7**, 60 310–60 331. (doi:10.18632/oncotarget.11203)
33. Hamburger V, Hamilton HL. 1951 A series of normal stages in the development of the chick embryo. *J. Morphol.* **88**, 49–92.
34. Summerhurst K, Stark M, Sharpe J, Davidson D, Murphy P. 2008 3D representation of Wnt and Frizzled gene expression patterns in the mouse embryo at embryonic day 11.5 (Ts19). *Gene Expr. Patterns* **8**, 331–348. (doi:10.1016/j.gep.2008.01.007)
35. Hartmann C, Tabin CJ. 2000 Dual roles of Wnt signaling during chondrogenesis in the chicken limb. *Development* **127**, 3141–3159.
36. Hartmann C, Tabin CJ. 2001 Wnt-14 plays a pivotal role in inducing synovial joint formation in the developing appendicular skeleton. *Cell* **104**, 341–351. (doi:10.1016/S0092-8674(01)00222-7)
37. Witte F, Dokas J, Neuendorf F, Mundlos S, Stricker S. 2009 Comprehensive expression analysis of all Wnt genes and their major secreted antagonists during mouse limb development and cartilage differentiation. *Gene Expr. Patterns* **9**, 215–223. (doi:10.1016/j.gep.2008.12.009)
38. Martin A, Maher S, Summerhurst K, Davidson D, Murphy P. 2012 Differential deployment of paralagous Wnt genes in the mouse and chick embryo during development. *Evol. Dev.* **14**, 178–195. (doi:10.1111/j.1525-142X.2012.00534.x)
39. Zhong Z *et al.* 2012 Wntless functions in mature osteoblasts to regulate bone mass. *Proc. Natl Acad. Sci. USA* **109**, E2197–E2204. (doi:10.1073/pnas.1120407109)
40. Kato K, Bhattaram P, Penzo-Méndez A, Gadi A, Lefebvre V. 2015 SOXC transcription factors induce cartilage growth plate formation in mouse embryos by promoting noncanonical WNT signaling. *J. Bone Miner. Res.* **30**, 1560–1571. (doi:10.1002/jbmr.2504)
41. Koyama E, Ochiai T, Rountree RB, Kingsley DM, Enomoto-Iwamoto M, Iwamoto M, Pacifici M. 2007 Synovial joint formation during mouse limb skeletogenesis: roles of Indian hedgehog signaling. *Ann. NY Acad. Sci.* **1116,** 100–112. (doi:10.1196/annals.1402.063)
42. Hyde G, Boot-Handford RP, Wallis GA. 2008 *Col2a1* lineage tracing reveals that the meniscus of the knee joint has a complex cellular origin. *J. Anat.* **213**, 531–538. (doi:10.1111/j.1469-7580.2008.00966.x)
43. Ozpolat BD, Zapata M, Fruge JD, Coote J, Lee J, Muneoka K, Anderson R. 2012 Regeneration of the elbow joint in the developing chick embryo recapitulates development. *Dev. Biol.* **372**, 229–238. (doi:10.1016/j.ydbio.2012.09.020)
44. Nowlan NC, Dumas G, Tajbakhsh S, Prendergast PJ, Murphy P. 2012 Biophysical stimuli induced by passive movements compensate for lack of skeletal muscle during embryonic skeletogenesis. *Biomech. Model. Mechanobiol.* **11**, 207–219. (doi:10.1007/s10237-011-0304-4)
45. Roddy KA, Kelly GM, van Es MH, Murphy P, Prendergast PJ. 2011 Dynamic patterns of mechanical stimulation co-localise with growth and cell proliferation during morphogenesis in the avian embryonic knee joint. *J. Biomech.* **44**, 143–149. (doi:10.1016/j.jbiomech.2010.08.039)
46. Ruano-Gil D, Nardi-Vilardaga J, Teixidor-Johe A. 1985 Embryonal hypermobility and articular development. *Acta Anat.* **123**, 90–92. (doi:10.1159/000146045)
47. Cha SW, Tadjuidje E, Tao Q, Wylie C, Heasman J. 2008 Wnt5a and Wnt11 interact in a maternal Dkk1-regulated fashion to activate both canonical and non-canonical signalling in *Xenopus* axis formation. *Development* **135**, 719–3729. (doi:10.1242/dev.029025)
48. van Amerongen R, Fuerer C, Mizutani M, Nusse R. 2012 Wnt5a can both activate and repress Wnt/β-catenin signaling during mouse embryonic development. *Dev. Biol.* **369**, 101–114. (doi:10.1016/j.ydbio.2012.06.020)